Effect of the Aspect Ratio on the heat transfer enhancement by the Al_2O_3-H_2O Nanofluid traversing a Heated Shallow Cavity

CHAHRAZED ABDELLAHOUM[1, 2], AMINA MATAOUI[2]

[1]Faculty of Sciences, M'hamed Bougera Universiy – Boumerdes, UMBB, ALGERIA
[2]Theoretical and Applied Fluid Mechanics Laboratory, University of Science and Technology Houari Boumediene — USTHB, ALGERIA

Abstract: - In this work, the effects of the cavity aspect ratio (AR) on the flow of Al_2O_3-water nanofluid in a two-dimensional cavity subjected on its lower part to a constant and uniform temperature. The governing equations are discretized by the finite volume method based one point closure turbulence model. For nanofluid proprieties, Maxwell-Garnetts model (MG) and Brinkman models are used for the calculation respectively of the conductivity and viscosity of the nanofluid. The parameters of this study are the shape parameter of the cavity from 2 to 14, Reynolds number Re between 4.10^3 and 10^5 and volume fraction of the nanoparticles between 0 and φ =4%. The cavity aspect ratio effect on the flow structure and heat transfer was also examined. The results confirm that the flow structure and heat transfer are very sensitive to the cavity aspect ratio. The numerical results highlight the effect of the main parameters on the distribution of Nusselt number and friction coefficient.

Key-Words: - Forced convection; cavity; heat transfer enhancement; nanofluids

Received: July 15, 2021. Revised: February 17, 2022. Accepted: March 19, 2022. Published: April 21, 2022.

1 Introduction

The open cavity in a channel flow is considered as an interesting topic for many researchers since it includes the phenomena of separation and reattachment in several engineering applications such as cooling of electronic components, solar collector, heat exchanger and nuclear reactors. Until now, the open cavity and the step flow interest many researchers to study heat transfer required in several industrial applications. According to the Plentovich classification, there is two distinct types of cavity flows, namely, open cavity of ($1 \leq AR \leq 8$) and closed cavity ($12 \leq AR \leq 14$). The cavity of aspect ratio AR = 10 is called transitional cavity flow. Although their geometrical simplicity, cavity flows are complex; they consists of complex flow phenomena. Nevertheless, this flow has been extensively studied, both experimentally and numerically, and has received considerable attention ever since the early work of Krishnamurty [1] and Roshko [2]. However, the flow over a rectangular cavity has been well described by Roshko [2] through the results of pressure and mean velocity measurements. Plentovich [3] investigations included pressure measurements for two different upstream boundary layer thicknesses. Its results indicate that as the boundary layer thickness decreases, positive pressure levels inside the cavity increase. Zdanski et al. [4] numerically simulated both laminar and turbulent flows over shallow rectangular cavities. They studied the influence of cavity aspect ratio, turbulence intensity of the incoming flow and Reynolds number. However the reattachment phenomenon mainly depends on the aspect ratio of the cavity, the experiments revealed that this phenomenon is also sensitive to the characteristics of the incident flow. A similar phenomenon was observed by several researchers. Eaton and Johnston [5] showed that the increase in the Reynolds number induces a reduction of the reattachment length and an important increase in the size of the recirculation zone. Several numerical and experimental works have been carried out to study the hydrodynamic and thermal behavior in confined flows. In this view, Manca et al. [6] studied numerically the effect of heated wall position on mixed convection in a channel with an open cavity. They took into account three heating modes as assisting flow, opposing flow and heating from below by applying constant heat flux. In their configuration, there is no inlet section and it suddenly extends to the cavity. After that, Manca et al. [7] investigated experimentally the mixed convection in an open cavity with the

heated vertical left wall at uniform heat flux. Atashafrooz et al. [8] studied laminar forced convection of gas flow over a recess including two backward and forward facing steps in a horizontal duct subjected to bleeding condition. The effects of bleeding coefficient and recess length on the flow and heat transfer behaviors of the system are investigated. Because of the efficiency of thermal properties of nanofluids, they were widely studied in the last decade for various flow configurations and different heat transfer processes. Oztop et al. [9] have performed a numerical study to analyze the effect of different nanofluids on the distribution of temperature field in a rectangular cavity. They confirmed that the increase of Rayleigh number and the volume fraction of the nanofluids improve significantly heat transfer. Al-aswadi et al. [10] investigated numerically the laminar forced convection flow over confined BFS using different nanofluids. They confirmed that the recirculation size and reattachment length increase as the Reynolds number increases in the laminar regime. A great number of experimental studies have focused on heat transfer behavior in a backward facing step flow. These configurations were performed under different conditions, which justify the absence of an accurate database for comparisons to confirm the best methodology to solve such problems. Xuan and Li [11] have investigated experimentally the turbulent convective heat transfer of a single phase flow of water–Cu nanofluids in straight heated tubes with a constant heat flux. Their results showed that nanofluids gave a substantial enhancement of heat transfer rate compared to the case of pure water. Kalteh et al. [12] have studied numerically and experimentally the convective heat transfer of a laminar flow of a water–Al2O3 nanofluid inside a rectangular micro channel heat sink subjected to a constant heat flux. Their experiments were done on pure water, 0.1% and 0.2% fraction volume of alumina–water nanofluid. They investigated the effect of Reynolds number and nanofluid volume fraction on heat transfer. Abdellahoum et al. [13] examined several models of the viscosity of turbulent forced convection of Al2O3 nanofluid over a heated cavity in a horizontal duct. They found that this work leads to further investigations for viscosity of nanofluids in forced convection in separated flow, experimentally and numerically.

Abdellahoum et al. [14] investigated the effect of nanoparticle volume fraction on thermal conductivity of nanofluid with nanoparticle volume fraction range between 0% and 4% and presented new correlations. According to results with increasing the nanoparticle volume fraction, the thermal conductivity of nanofluid increases.

This study extends previous work (Abdellahoum et al. [14]) and aims to analyze numerically the hydrodynamic and thermal aspect of a turbulent single-phase flow of a nanofluid composed of solid particles of alumina (Al2O3) dispersed in a base fluid (pure water) for different aspect ratios.

The main aim of this study is to investigate turbulent heat transfer in a channel with cavity

2 Physical Model

Turbulent forced convection of nanofluid flow in a heated cavity is numerically simulated. The flow is assumed as Newtonian, steady in average and incompressible. A schematic of the cavity with coordinates and boundary conditions are sketched in Figure 1.

The bottom of the cavity is heated to a constant temperature (Tw > T0), while the confining wall is adiabatic. The base fluid (i.e. water) and the nanoparticles are in thermal equilibrium and no slip boundary condition occurs between them. Thermophysical properties of the Al2O3 nanofluid are assumed to be constant.

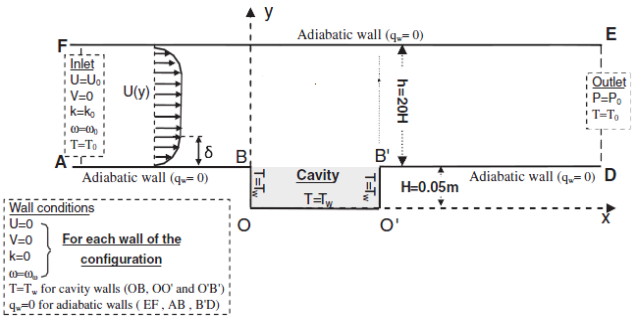

Fig. 1. Sketch of the problem geometry and boundary conditions.

In this study, the applied models for thermophysical properties of the nanofluid are given in table 1.

Table 1 Applied models for thermophysical properties of the nanofluid and hybrid nanofluid

Property	Nanofluid
Density	$\rho_{nf} = (1-\varphi)\rho_f + \varphi\rho_s$
Dynamic viscosity	$\mu_{nf} = \frac{\mu_f}{(1-\varphi)^{2.5}}$
Thermal conductivity	$\frac{k_{nf}}{k_f} = \frac{k_s + 2k_f + 2\varphi(k_s - k_f)}{k_s + 2k_f - \varphi(k_s - k_f)}$
Heat capacity	$C_{p_{nf}} = \frac{(1-\varphi)(\rho C_p)_f + \varphi(\rho C_p)_s}{\rho_{nf}}$

Before starting the discussion of the results of the simulation in the cavity, we give in the table 2 the thermophysical characteristics of base fluid and the nanoparticle used in this work.

3. Governing equation

The governing equations for a homogenous analysis of forced convection are continuity (eq. 1), momentum (eq. 2), and Energy (eq. 3) depending on their nanofluid properties, as follows:

$$\frac{\partial U_i}{\partial x_i} = 0 \tag{1}$$

$$\rho_{nf} U_j \frac{\partial U_i}{\partial x_j} = -\frac{\partial P}{\partial x_i} + \frac{\partial}{\partial x_j}\left(\mu_{nf}\frac{\partial U_i}{\partial x_j} - \rho_{nf}\overline{u_i u_j}\right) \tag{2}$$

$$\rho_{nf} U_i \frac{\partial T}{\partial x_i} = \frac{\partial}{\partial x_i}\left(\frac{\mu_{nf}}{p_{r_{nf}}}\frac{\partial T}{\partial x_i} - \rho_{nf}\overline{u_i\theta}\right) \tag{3}$$

In the above equations, the symbols U_i, P and T correspond to the time averaged flow variables, while u_i and θ represent the fluctuations of velocity and temperature. The turbulent shear stress $\overline{u_i u_j}$ and turbulent heat flux $\overline{u_i\theta}$, require modeling. They may be approximately expressed versus the time averaged flow variables (velocity or temperature) . By analogy with molecular transport, for all models (first or second order models), the Simple Gradient Diffusion Hypothesis (SGDH) is used. The following algebraic constitutive law is allows to deduce the velocity-temperature correlation are deduced by the following algebraic equations which based on the Boussinesq assumption.

$$\overline{\rho_{nf} u_i u_j} = \frac{2}{3}\rho_{nf} k\delta_{ij} - \mu_t(U_{i,j} + U_{j,i}) \tag{4}$$

$$-\rho_{nf}\overline{u_i\theta} = \alpha_t \frac{\partial T}{\partial x_i} \tag{5}$$

Although the nanofluids are solid-liquid mixtures, the approach conventionally used in most studies of forced convection handles the nanofluid as a single-phase (homogenous) fluid. In fact, due to the extreme size and low concentration of the suspended nanoparticles, the particles are assumed to move with same velocity as the fluid.

4. Grid arrangement and validation

The two-dimensional Cartesian coordinate system is used to simulate flow by considering non-uniform structured grid. Sufficiently fine grids are in the viscous sub-layer, near each wall where a very high gradient of variables prevail (Fig. 2). For each cavity ratio , a grid is generated as shows Figure 2.

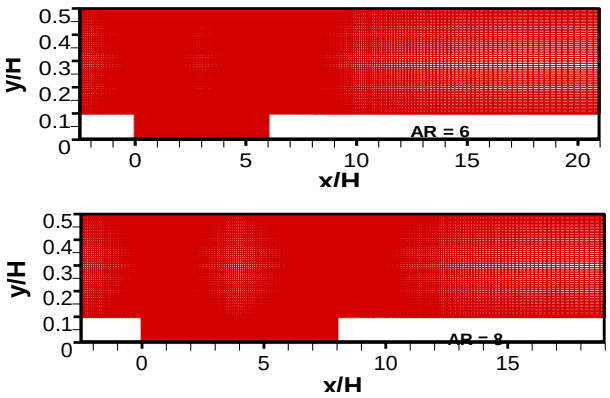

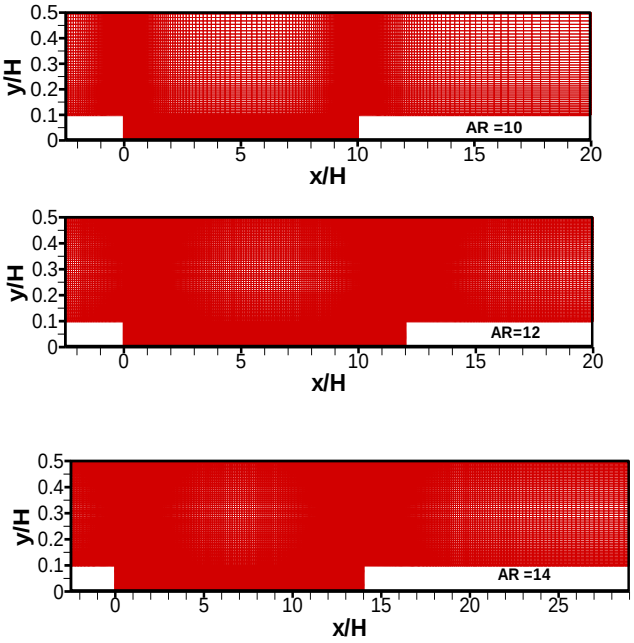

Fig. 2. Typical grid of (x, y) plane for each cavity aspect ratio.

For each case a grid independency test is carried out by refining and adjusting the grid in the two directions. For each grid, the heat transfer characteristics are examined for a wide range of aspect ratios and Reynolds numbers. In order to ensure the accuracy as well as the consistency of numerical results, several non uniform grids have been tested for each of all considered cases.

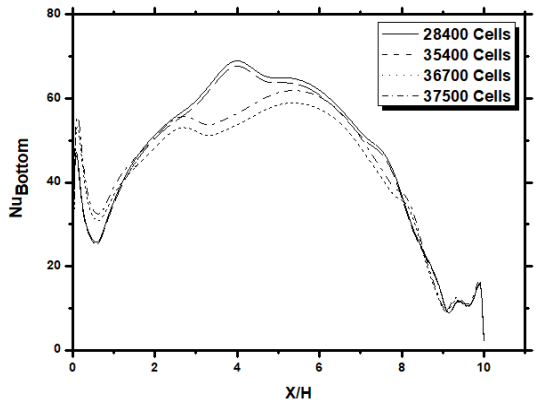

a) Local Nusselt number

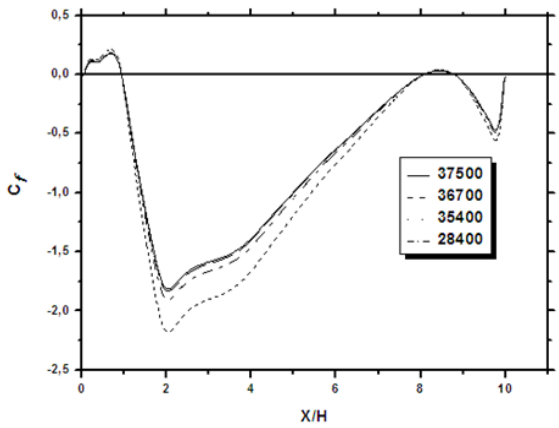

b) Local Friction coefficient

Fig. 3. Typical grid test : AR = 10, Re = 6.10^4.

As shows Fig. 3, a good overall agreement was obtained between grid 3 (36,700 cells) and Grid 4 (37,500 cells). Grid 3 gives satisfactory results on the number of Nusselt and the coefficient of friction. The numerical results of the present study are carried out by the grid 3 since the geometrical parameters remain unchanged; and to reduce the calculation time.

5. Validation

This study extends the previous work of Abdellahoun et al. [13] by considering several viscosity models on water–Al2O3 nanofluids at small volume particle fraction. The influence of nanoparticle. For validation the pressure coefficient along the cavity bottom is compared to experimental data of numerical predictions of Arous et al. [17] and Esteve et al. [18]. An overall good agreement is obtained as shown in Fig. 4. One notes that pressure distribution varies from a concave-up shape to a concave-down shape. Therefore, Fig. 4 confirms that a cavity of an aspect ratio of 10 corresponds to an open cavity according to the classification of Plentovich (Plentovich et al. [19]).

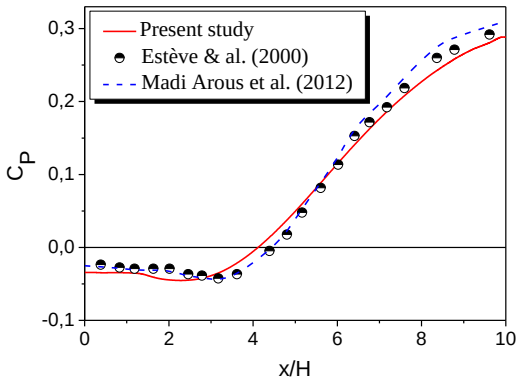

Fig. 4. Validation

Pressure coefficient distribution along the cavity bottom (Re =10^5, AR = 10).

6. Results and discussion

This part presents the results obtained by the numerical simulation applied to a turbulent flow of nanofluid through a shallow cavity. The water–Al2O3 nanofluid is considered as the working fluid in this article. The influence of aspect ratios and the Reynolds number on the flow fields and heat transfer were examined. The geometry gives rise to the appearance of complex vortex structures. Characterized by a main recirculation zone delimited by the attachment length which corresponds to the point where the shear layer joins the lower solid wall of the cavity. Figures 5 shows the topology of the flow inside the cavity obtained with k-ω SST turbulence model for a mixture containing 4% of the nanoparticles (φ = 4%). These figures are characterized by the presence Contra-rotating vortices at the level of the walls. It's about respectively of the main recirculation zone (Primary) and secondary recirculations. The turbulent boundary layer takes off at the upstream edge of the cavity giving birth to a shear layer and thereby creating a first recirculation zone having high average velocity gradients, then separates again just before the downstream wall, Thus creating a foot whirl. By analyzing the flow through these structures, we observe the presence of three vortex structures in the cavities of large aspect ratios (AR = 14, 12 and 10). The corner vortices grow in size as aspect ratio increases. In the case of the cavity of aspect ratio equal to 8, the main recirculation bubble touches the one that is in front of the downstream step. We also note the presence of a vortex located at the upstream corner and the total disappearance of the vortex located on the downstream step. For AR=6, the main tourbillion merges with the secondary vortex thus forming a single recirculation bubble.

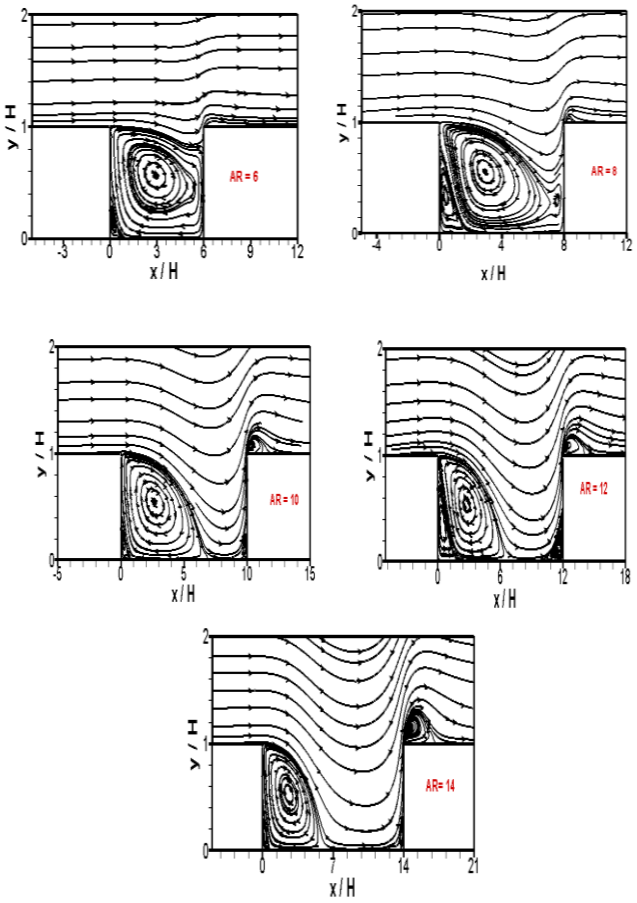

Fig. 5. Streamlines contours : effect of cavity aspect ratio (Re = 10^5,φ = 4%).

The pressure coefficient makes it possible to classify the flows of cavities and to examine the overall characteristics of the flow. Figure 6 illustrate the evolution of the static pressure coefficient along the lower wall of the cavities as a function of the longitudinal distance. It can be noticed that pressure distribution varies from a concave-up shape to a concave down shape. In the case of cavities with large aspect ratios , the pressures are more important while the cavities of small aspect ratios are characterized by lower wall pressures. According to the classification of Plentovich [20], the flow of the cavity with an aspect ratio of 14, is that of a closed cavity. Whereas the cavity of aspect ratio of 6, 8, 10 and 12, the flow is that of an open cavity.

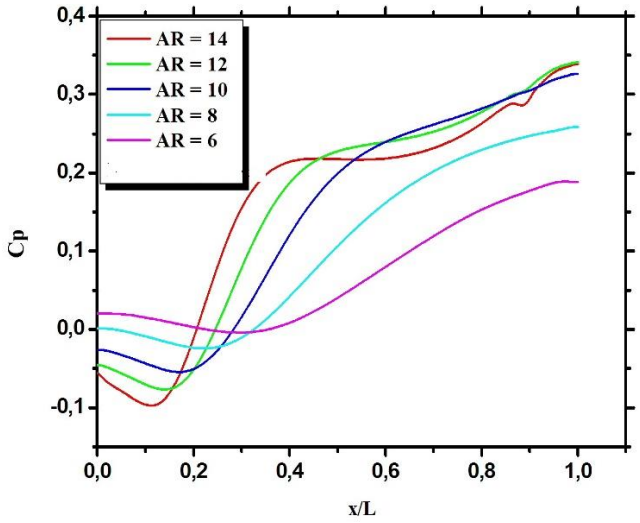

Fig. 6. Pressure coeffecient along the cavity bottom: effect of aspect ratio (Re = 10^5, φ = 4%).

Figure 6 highlights the influence of aspect ratio on the pressure coefficient at the bottom of the cavity. The pressure distribution, In the case of the cavity having an aspect ratio of 6, 8 and 10, does not show a change in concavity. It is seen from these results that the pressure distribution is sensitive to the changes of the aspect ratios.

In all cases, there is a negative pressure on the step face followed initially by slight drop in pressure downstreamof the step, and then by a rather rapid rise of pressure indicating the reattachment of separated flow. The base pressure is essentially the same for different cavities and the pressure rise by reattachement increases slihtly as the aspect ratio increases

The effect of the volume fraction, Reynolds number and cavities aspect ratios; are examined through the distribution of local and averaged Nusselt number.

For the each cavity wall (Bottom and side walls) in the test section through which the nanofluid flowed, the local Nusselt number was obtained using the computed values of the local heat transfer coefficient and is written as:

$$Nu_{Bottom}(x) = -\left(\frac{k_{nf}}{T_0 - T_w}\right)\left(\frac{\partial T}{\partial y}\right)_{ywall} \quad and \quad Nu_{side}(y) = -\left(\frac{k_{nf}}{T_0 - T_w}\right)\left(\frac{\partial T}{\partial x}\right)_{xwall} \tag{14}$$

Figure 7 depicts the effect of the nanoparticle volume fraction φ, Reynolds number Re and the aspect ratios AR, on heat transfer via the values of local Nusselt number along the cavity bottom. We notice that the curves have a similar shape. The increase of aspet ratio leads to an increase in the number of local Nusselt and a displacement of its maximum value downstream of the cavity. For all the cases tested, it reaches its maximum value which corresponds to the gluing area which is the seat of the best heat exchange hence the Nusselt number is much higher, Then, it falls to reach a minimum. We also find that all curves go through a minimum.

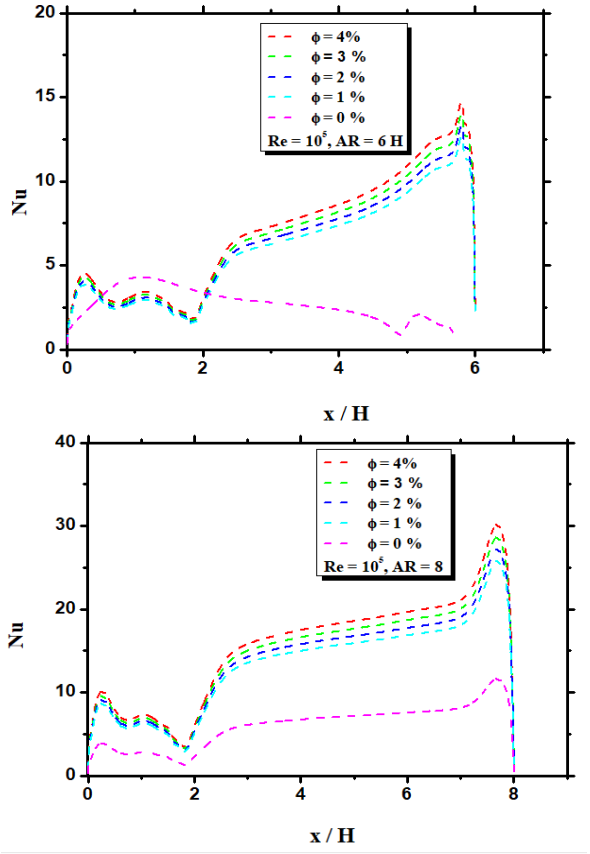

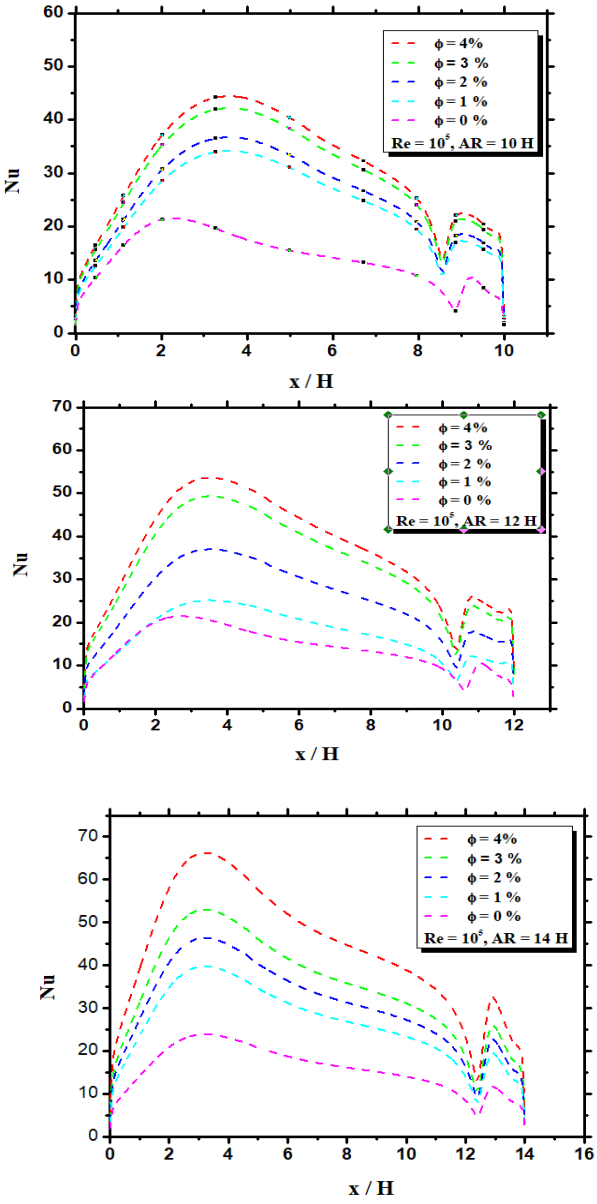

Fig. 7. Effect of the cavity aspect ratios on local Nusselt number along the cavity bottom.

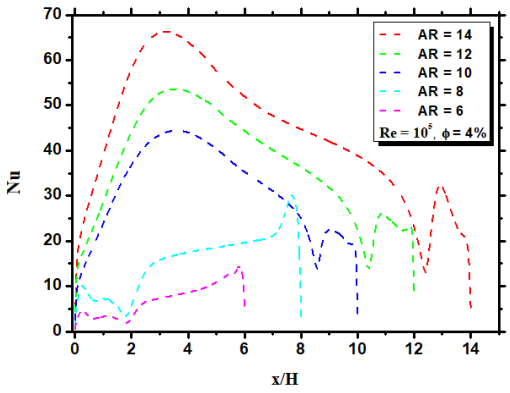

(a)

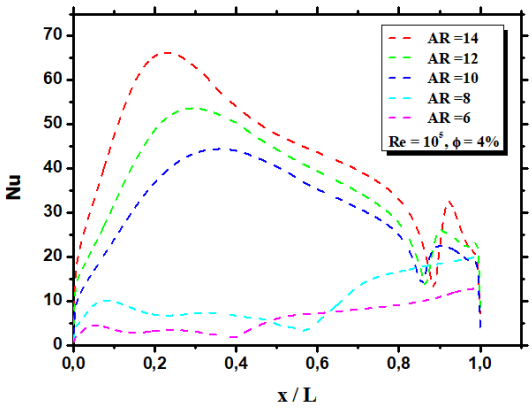

(b)

Fig. 8. Variation of local Nusselt number at the bottom cavity for different aspect ratios:

(a) Versus x/H, (b) Versus x/L.

Thermal exchanges for the flow of the nanofluid inside the cavity are characterized by the average Nusselt number which is determined from the following relation:

The effect of the aspect ratio on the average Nusselt number is shown in table 3.

It can be seen through this table that the average Nusselt number undergoes a noticeable increase for some aspect ratios. The maximum value of Nu is reached for the ratio AR = 14. In addition, the evolution of the average Nusselt number for a given Reynolds number and a volume fraction varies between 1% and 4%, shows that the smallest heat transfer values are obtained by the aspect ratio cavity AR = 6. So, we can conclude that the flow structure and the Nusselt number (Average and local) are strongly influenced by the geometrical characteristics used Abdellahoum et al [21].

Table 3. Average Nusselt number for différent values of the aspect ratios

Re = 10^5						
AR		6H	8H	10H	12H	14H
Nu Avg	Nanofluids	19,66	20,69	24,34	28,40	28,47
	Pure water	11,97	12,60	14,82	17,296	17,34

In the light of this study, we established global correlation quantifying the average Nusselt number depending on the different characteristic parameters namely Reynolds number,nanoparticle volume fraction and the aspect ratio. This correlation is valid for a range of Reynolds number ranging from 40000 to 100000 and a nanoparticles volume fraction of 0≤φ≤2%.

$$\overline{Nu} = \left(0.00033767 AR^{0.502} + 0.028\,\varphi^{1.23}\right).\mathrm{Re}^{0.834}$$

A good agreement between this correlation and the numerical results is observed at the level of the Figure 9.

This figure compares the evolution of the average Nusselt number for numerical predictions and with the proposed correlation for each cavity. We note a concordance quite satisfactory for all the cases studied.

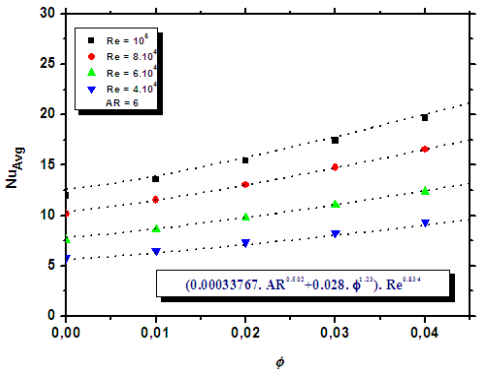

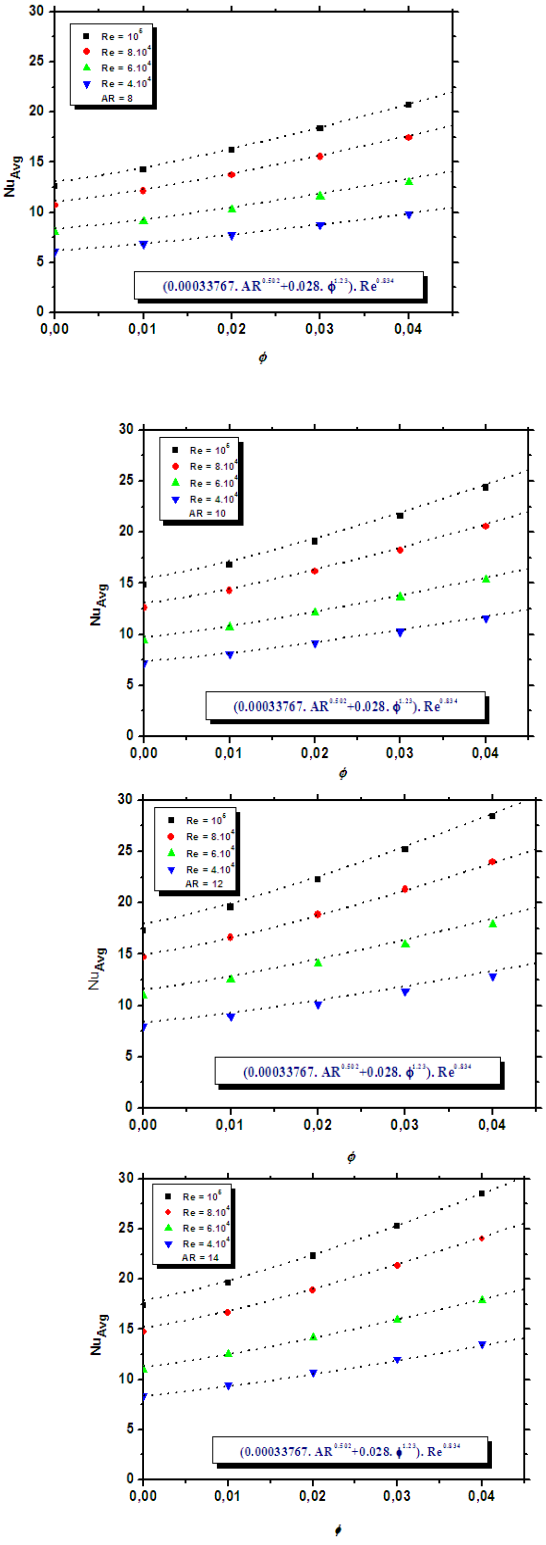

Fig.9. Average Nusselt number versus nanoparticle volume fraction ϕ, Reynolds number and aspect ratio AR.

7. Conclusion

Based on the finite volume method, we first described and validated the numerical method by referring to the previous results. Then, the focus is on studying the thermal and dynamic fields of turbulent flow in forced convection. In particular, we studied the effects of different parameters on the flow and heat transfer induced by two-dimensional forced convection within a rectangular cavity heated from below. Comparisons were made according to different criteria by using previous results.

In conclusion the results have clearly show that :

1- The pressure rise by reattachement increases slihtly as the aspect ratio increases
2- maximum heat transfer is achieved at the point of attachment followed by a decrease towards the zone of fully developed flow.
3- The local Nusselt number is low in the recirculation zone and that it is maximal at the point of recollement, and this maximum increases with increasing Reynolds number.
4- he increase of aspect ratio enhances heat transfer, for each nanoparticle volume fraction

References:

[1] Krishnamurty K., 1955, Acoustic radiation from two-dimensional rectangular cutouts in aerodynamic surfaces. NACA, Tech. Note 3487.
[2] A. Roshko A., 1955, Some measurements of flow in a rectangular cutout. NACA Technical Note, No. 3448.
[3] Plentovich E. B., 1990, three dimensional cavity flow fields at subsonic and transonic speeds. NASA, TM-4209.
[4] Zdanski P. S. B, Ortega M. A., Nide G. C. R. et Fico, Tr., 2003, Numerical study of the flow over shallow cavities, Computers & Fluids, vol. 32, (7), pp. 953-974.
[5] Eaton J. K. & Johnston J. P., 1981, A review of research on subsonic turbulent flow reattachment, AIAA, vol. 19, pp. 1093-1099.
[6] O. Manca, S. Nardini, K. Vafai, Experimental investigation of mixed convection in a channel with an open cavity, Exp. Heat Transf. 19 (2006) 53–68.
[7] O. Manca, S. Nardini, K. Khanafer, K. Vafai, Effect of heated wall position on mixed convection in a channel with an open cavity, Numer. Heat Transf., Part A 43 (2003) 259–282.
[8] M. Atashafrooz, S. Abdolreza Gandjalikhan Nassab, A. Babak Ansari, Numerical investigation of entropy generation in laminar forced convection flow over inclined backward and forward facing steps in a duct under bleeding condition, Therm. Sci. 18 (2014) 479–492.
[9] H.F. Oztop, Eiyad Abu-Nada, Numerical study of natural convection in partially heated rectangular enclosures filled with nanofluids, Int. J. Heat Fluid Flow 29 (2008) 1326–1336.
[10] A.A. Al-aswadi, H.A. Mohammed, N.H. Shuaib, A. Campo, Laminar forced convection flow over a backward facing step using nanofluids, Int. Commun. Heat Mass Transf. 37 (2010) 950–957.
[11] Y. Xuan, Q. Li, Investigation on convective heat transfer and flow features of nanofluide, J. Heat Transf. 125 (2003) 151–155.
[12] M. Kalteh, A. Abbassi, M. Saffar-Avval, Jens Harting, A. Darhuber, J. Harting, Experimental and numerical investigation of nanofluid forced convection inside a wide microchannel heat sink, Appl. Therm. Eng. 36 (2012) 260–268.
[13] C. Abdellahoum, A. Mataoui, H.F. Oztop, Turbulent forced convection of nanofluid over a heated shallow cavity in a duct, Powder Technol. 277 (2015) 126–134.
[14] C. Abdellahoum , A. Mataoui, H.F. Oztop., Comparison of viscosity variation formulations for turbulent flow of Al2O3–water nanofluid over a heated cavity in a duct, Advanced Powder Technology (2015),
[15] F.R. Menter, 'Two-equation eddy-viscosity turbulence models for engineering applications, AIAA J. 32 (1994) 1598–1605.
[16] D.C. Wilcox, Turbulence Modeling for CFD, DCW Industries Inc, La Canada, California, 1994.
[17] F. Madi Arous, A. Mataoui, Z. Bouahmed, Influence of upstream flow characteristics on the reattachment phenomenon in shallow cavities, Therm.Sci. – Int. Sci. J. 15 (2011) 721–734.
[18] M.J. Estève, P. Reulet, P. Millan, Flow field characterisation within a rectangular cavity, in: 10th International Symposium on Applications of Laser Techniques to Fluid Mechanics, Lisboan, Portugal, 2000.
[19] Plentovich E. B., Stallings Jr R. L. & Tracy M. B., 1993, Experimental cavity pressure

measurements at subsonic speeds, Nasa Technical Paper, Technical report 3358.
[20] Plentovich E. B., 1990, three dimensional cavity flow fields at subsonic and transonic speeds. NASA, TM-4209.
[21] Abdellahoum. C, Mataoui.A. Forced Convection of Nanofluid Flow Over a Heated Shallow Cavity. Journal of Nanofluids. 4 (2015) 1-9.